

図 5. DNA-DNA hybridization 法(国立感染症研究所 中永和枝博士提供)
M. marinum に陽性を示している。

る。病原体検出には、Z-N 染色(図 4-c)や蛍光染色(図 4-d)が用いられる。

4. 分子生物学的検査

a) 核酸増幅法(PCR 法)

膿汁や組織などの臨床検体、培養したコロニーを材料とし、DNA を抽出し、PCR により増幅し、目的とする菌の特異的遺伝子配列を抽出する方法である。Amplicor Mycobacterium など数種の診断キットがあり、保険適応になっている。Amplicor では *M. tuberculosis complex*, *M. avium* および *M. intracellulare* の検出・同定が可能である。ブルーリ潰瘍の原因菌である *M. ulcerans* については、日本ではその亜種である *M. ulcerans* subsp.(subsp.) *shinshuense* が分離同定されている。ほとんどの患者には海外渡航歴がないことから、この亜種は日本あるいはアジア特有の *M. ulcerans* と考えられている。*M. ulcerans* subsp. *shinshuense* の同定のためには生検組織、培養検体、パラフィン切片からの PCR より特異的 DNA である IS2404 を検出する必要がある³⁾。本疾患の一連の検査については、国立感染症研究所ハン

セン病研究センターで行っている。

b) DNA-DNA hybridization 法

DDH 法とは、DNA 配列間の類似性を評価することにより、菌の同定を行う分子生物学的検査である。培養したコロニーから DNA を抽出し、一本鎖にして、各菌に特異的な DNA とハイブリダイゼーション(結合)させることにより、類似性を比較する。DDH マイコバクテリア(極東製薬)が代表的で、計 18 種の抗酸菌の鑑別が可能である(図 5)。しかし、交叉反応を示す菌種があり、例えば、*M. ulcerans* は *M. marinum* と同一ウェルで陽性になるため、注意が必要である。

以上をまとめ、主要な抗酸菌を診断するために有効な検査法を表 4 に示した。

5. その他

a) ツベルクリン反応(ツ反)

Purified protein derivative(PPD)という抗原を皮内注射し、48 時間後の反応を判定する。10 mm 以上の発赤があれば弱陽性、10 mm 以上の発赤かつ硬結があれば中等度陽性、それよりも強い反応(水疱、壊死など)があれば強陽性と判定する。し

表 4. 主な抗酸菌の検査のまとめ(文献 2 より一部改変して転載)

抗酸菌名	塗沫検査	病理組織検査 (抗酸菌染色)	培養	PCR	DNA-DNA hybridization (培養成功例)	備考
<i>M. tuberculosis</i>	○	○	○	外注 (膿汁)	○	結核疹は菌陰性, PCR で陽性の ときあり
<i>M. bovis</i> BCG	○	○	○	研究室レベル	○	Id 疹は菌陰性
<i>M. leprae</i>	○	○ (Fite 法)	×	依頼 (組織)	×	少菌型(I, TT, 一部 BT 型)では 菌陰性あるいは少数, PCR で陽 性のときあり
<i>M. marinum</i>	○	○	○ 室温でも培養	依頼 (組織)	○	感染源からの菌の同定
<i>M. ulcerans</i>	○	○	○ 32℃でも培養	依頼 (膿汁, 組織)	×	日本では亜種の <i>M. ulcerans</i> subsp. <i>shinshuense</i> 同定 マイコラクトン(脂質毒素)の産生
<i>M. avium</i>	○	○	○ 40℃でも培養	外注 (膿汁, 組織)	○	感染源からの菌の同定
<i>M. fortuitum</i>	○	○	○ 室温でも培養	外注 (膿汁, 組織)	○	感染源からの菌の同定

表 5. QFT-3G と T-スポット®. TB の比較

	QFT-3G	T-スポット®. TB
試料	全血(3ml), 専用の採血管	全血(2~8ml), ヘパリン入り採血管
検査方法	全血を抗原で刺激し IFN- γ を ELISA 法で 測定	全血から単球を分離し, IFN- γ 産生 T 細胞 数を ELISPOT 法で測定
検査使用抗原	ESAT-6, CFP-10, TB 7.7	ESAT-6, CFP10
小児への適応	中学生以上に適用されるべき	あり
感度	92.6%	97.5%
特異度	98.8%	99.1%
他の抗酸菌での陽性の可能性	<i>M. kansasii</i> , <i>M. leprae</i> , <i>M. marinum</i> , <i>M.</i> <i>szulgai</i> , <i>M. ulcerans</i> など	<i>M. gordonae</i> , <i>M. kansasii</i> , <i>M. leprae</i> , <i>M.</i> <i>marinum</i> , <i>M. szulgai</i> , <i>M. ulcerans</i> など
承認	2009年4月	2012年11月
保険点数	630点+144点(判断料)	630点+144点(判断料)

かし、結核菌の加熱滅菌培養液を粗精製して作られるため、さまざまな抗原の混合であり、結核菌以外の *M. bovis* BCG や NTM の抗原との相同性があり交叉する。抗酸菌のスクリーニング検査として有用であるが、BCG 接種が国民全員に実施されている日本では、結核感染検査の判定には慎重を要する。

b) 内臓病変の検査

感染症である本疾患群では、内臓にも病巣を有している可能性がある。特に、皮膚結核が発見された場合には、胸部 X 線検査、CT 検査、喀痰検査、胃液検査などを行い、肺内病変、その他の内臓・骨などに病変がないかの確認を行う必要がある。

c) 神経学的検査

ハンセン病では、末梢神経の検査が必須である(「ハンセン病の検査」の稿参照)。

d) 抗 PGL-I 抗体

ハンセン病患者での末梢血を用いた検査で、らい菌の菌体外に分泌される PGL-I (phenolic glycolipid-I) に対する抗体を検出する方法である。

e) インターフェロン- γ 遊離試験 (Interferon-Gamma Release Assay ; IGRA)

末梢血を結核菌に特異的な抗原で刺激し、結核菌に対する免疫応答を調整するサイトカインである interferon gamma (IFN- γ) を検出する結核の補助的診断方法である。クオンティフェロン検査と ELISPOT 検査がある(後述)。

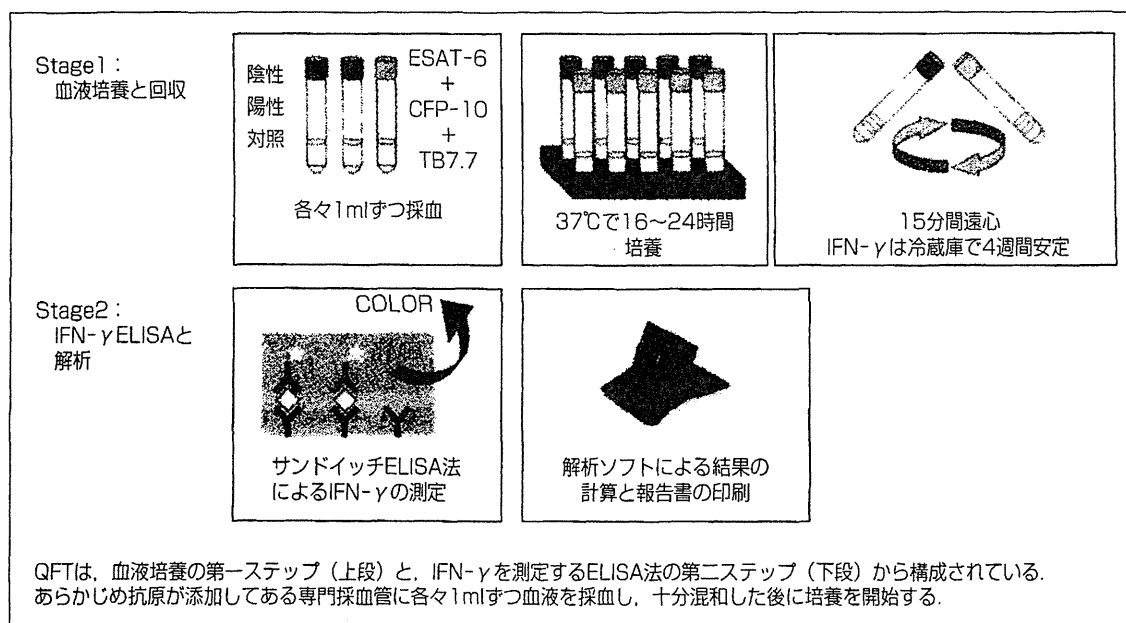


図 6. クォンティフェロンの検査手順(文献6より改変して転載)

表 6. クォンティフェロンの測定値の解釈(文献6より転載)

測定値 M(IU/ml)	測定値 A(IU/ml)	結果	解釈
不問	0.35 以上	陽性	結核感染を疑う
0.5 以上	0.1 以上 0.35 未満	判定保留	感染リスクの度合いを考慮し、総合的に判断する
	0.1 未満	陰性	結核感染していない
0.5 未満	0.35 未満	判定不可	免疫不全などが考えられるので、判定を行わない

測定値 A=結核抗原刺激血漿の IFN-γ 濃度-陰性コントロール血漿の IFN-γ 濃度

測定値 M=陽性コントロール血漿の IFN-γ 濃度-陰性コントロール血漿の IFN-γ 濃度

これらの測定値を結果の希釈に用いる。

クォンティフェロン検査^{5)~10)}

クォンティフェロン®TB-3 G(QuantiFERON® TB-3rd Generation; QFT-3 G, 海外では QFT®-Gold In-Tube: QFT-GIT)が結核の検査として2009年4月に保険適用になった(表5)。QFT-3 Gは小児期のBCG接種の影響を受けずに、結核菌に特異的な抗原 ESAT-6, CFP-10 や TB 7.7 に対する細胞性免疫能(IFN-γ産生)を指標にした検査キットで、結核特異抗原が加えられた検査チューブ(専用採血管)にて採血後16~24時間培養し、上清中に活性化T細胞から分泌されたIFN-γをELISA法にて検出する(図6)⁶⁾。結核感染に特異的な検査法として使用されている。QFT検査の測定値の判定法を、表6⁶⁾に示す。結

核に感染してからQFTが陽性になるまでの期間は2~3か月と考えられており、結核においては感度92.6%、特異度98.8%と信頼度の高い検査である。

一方、*M. bovis* BCGはESAT-6, CFP-10やTB7.7を持っていないが一部のNTMは持っているものもあり、結核のみならず他の抗酸菌感染症に対してどのような反応を示すかは、まだ不明である。症例報告レベルでは、皮膚結核においてQFT陽性例が散見されるが、内臓結核合併例がほとんどであり^{11)~13)}、データは十分でなく、今後の症例の蓄積が待たれる。

ELISPOT法¹⁴⁾¹⁵⁾

ELISPOT法は、QFT検査と同様に、結核感染

の有無を診断する IGRA 検査である(表 5)。2012 年 11 月に保険適応となった。検査キットである T-スポット[®]。TB は、対象者から採血して全血からリンパ球を分離し、抗ヒト IFN- γ 抗体をコーティングした polyvinylidene fluoride (PVDF) 膜などで底を覆った 96 穴培養プレートに、一定量を分注する。次に、結核菌特異抗原 ESAT-6 および CFP-10 を添加して、20 時間前後培養する。結核感染者の活性化 T 細胞は IFN- γ を分泌するため、細胞近傍の PVDF 膜上の抗ヒト IFN- γ 抗体と結合する。膜上に結合した IFN- γ を免疫染色法で染色すると活性化 T 細胞(IFN- γ を産生する細胞)があった部分がスポット状に染まるので、その個数を計測し、抗原刺激を行わないコントロールのスポットの個数との差を判定値として、結核感染を診断する。感度は 97.5%、特異度は 99.1%である。

QFT 検査同様、*M. bovis* BCG には交差性を示さないが、一部の抗酸菌には陽性の結果を示すことが分かっているため、他の検査法も併せて診断する。採血は、専用採血管が必要な QFT 検査と違い、通常のヘパリン入り採血管と簡便である一方で、検査自体の操作性はリンパ球の分離・調整の過程があり、QFT 検査よりも複雑である。特に QFT 検査で診断できないような、細胞性免疫が低下傾向にある人や小児での結核感染診断で期待が持たれている。QFT 検査同様、皮膚結核でのデータは乏しく、今後実用化にはデータや経験の蓄積が必要である。

さいごに

結核は、戦後、化学療法の進歩により減少したが、1980 年以降一時増加傾向にあり、再興感染症として位置づけられている。そのなかで、皮膚結核は年間約 100 症例の報告がある。ハンセン病は、30 年前は年間 50 例前後の日本人例があったが、最近では数例程度と、日本人にはほとんどみられない抗酸菌感染症となった。しかし、世界的にはまだ年間 23 万人の新規発症があり、最近の

日本でも在日外国人などの例は認められる。一方で、NTM 症は、近年 HIV 感染症や免疫抑制剤などの治療を受けている易感染性の患者の増加に伴い、発症の増加が懸念されている。皮膚抗酸菌症は、決して頻度の高い疾患ではないが、疑わなければ診断のできない疾患でもある。鑑別する目を養い、診断法を身につけ、正確な診断とそれに続く治療を行う能力が、臨床の現場で求められている。

文 献

- 1) 石井則久：皮膚抗酸菌症テキスト，金原出版，2008。
- 2) 石井則久，鈴木幸一：抗酸菌感染症．皮膚臨床，51(11)：1599-1606，2009。
- 3) Nakanaga K, Hoshino Y, Yotsu RR, et al : Laboratory procedures for the detection and identification of cutaneous non-tuberculous mycobacterial infections. *J Dermatol*, 40 : 151-159, 2013.
- 4) 石井則久：古くて新しい感染症．*Visual Dermatology*, 12(9)：918-922, 2013.
- 5) 常深祐一郎，石井則久：抗酸菌感染症．*MB Derma*, 206 : 27-37, 2013.
- 6) 森亨，原田登之，鈴木公典：平成 24 年改訂版現場で役立つクオンティフェロン TB ゴールド使用の手引き，公益財団法人結核予防会，2012。
- 7) 日本結核病学会予防委員会：クオンティフェロン TB ゴールドの使用指針．*結核*, 86(10)：839-844, 2011.
- 8) Matulis G, Juni P, Villiger PM, et al : Detection of latent tuberculosis in immunosuppressed patients with autoimmune diseases : performance of a *Mycobacterium tuberculosis* antigen-specific interferon gamma assay. *Ann Rheum Dis*, 67 (1) : 84-90, 2008.
- 9) Diel R, Loddenkemper R, Nienhaus A : Predictive value of interferon-gamma release assays and tuberculin skin testing for progression from latent TB infection to disease state : a meta-analysis. *Chest*, 142(1) : 63-75, 2012.
- 10) Diel R, Loddenkemper R, Niemann S, et al : Negative and positive predictive value of a whole-blood interferon-gamma release assay for developing active tuberculosis : an update. *Am J*

- Respir Crit Care Med*, 183(1) : 88-95, 2011.
- 11) Bryant PA, Shingadia DV : Lumps and bumps. *BMJ Case Reports*, 2009. Available at : doi : 1-1136/bcr.11.2008.1220.
 - 12) Angus J, Roberts C, Kulkarni K, et al : Usefulness of the QuantiFERON test in the confirmation of latent tuberculosis in association with erythema induratum. *Brit J Dermatol*, 157(6) : 1293-1294, 2007.
 - 13) Sharon V, Goodarzi H, Chambers CJ, et al : Erythema induratum of Bazin. *Dermatol Online J*, 16(4) : 1, 2010.
 - 14) 加藤誠也 : Tスポット®. TBについて. 複十字, 348 : 8-9, 2013.
 - 15) Lalvani A, Pareek M : Interferon gamma release assays : principles and practice. *Enferm Infecc Microbiol Clin*, 28(4) : 245-252, 2010.

RESEARCH ARTICLE

Open Access

An *in vitro* model of *Mycobacterium leprae* induced granuloma formation

Hongsheng Wang^{1,2}, Yumi Maeda^{2*}, Yasuo Fukutomi² and Masahiko Makino²

Abstract

Background: Leprosy is a contagious and chronic systemic granulomatous disease caused by *Mycobacterium leprae*. In the pathogenesis of leprosy, granulomas play a key role, however, the mechanisms of the formation and maintenance of *M. leprae* granulomas are still not clearly understood.

Methods: To better understand the molecular physiology of *M. leprae* granulomas and the interaction between the bacilli and human host cells, we developed an *in vitro* model of human granulomas, which mimicked the *in vivo* granulomas of leprosy. Macrophages were differentiated from human monocytes, and infected with *M. leprae*, and then cultured with autologous human peripheral blood mononuclear cells (PBMCs).

Results: Robust granuloma-like aggregates were obtained only when the *M. leprae* infected macrophages were co-cultured with PBMCs. Histological examination showed *M. leprae* within the cytoplasmic center of the multinucleated giant cells, and these bacilli were metabolically active. Macrophages of both M1 and M2 types co-existed in the granuloma like aggregates. There was a strong relationship between the formation of granulomas and changes in the expression levels of cell surface antigens on macrophages, cytokine production and the macrophage polarization. The viability of *M. leprae* isolated from granulomas indicated that the formation of host cell aggregates benefited the host, but the bacilli also remained metabolically active.

Conclusions: A simple *in vitro* model of human *M. leprae* granulomas was established using human monocyte-derived macrophages and PBMCs. This system may be useful to unravel the mechanisms of disease progression, and subsequently develop methods to control leprosy.

Keywords: Mycobacteria, Leprosy, Granuloma

Background

Leprosy is a chronic mycobacterial infection that presents an extraordinary range of cellular immune responses in humans. Regulation of cell-mediated immunity against *Mycobacterium leprae* through the fine-tuning between cells, cytokines and chemokines continues to be unraveled. Similar to other mycobacterial infections, granulomatous inflammation in the skin lesion defines certain forms of leprosy [1,2]. The bacilli enter and replicate within macrophages, resulting in the production of cytokines and chemokines, which in turn triggers an inflammatory response leading to the recruitment of macrophages and lymphocytes at the infectious site. Granulomas mainly contain

macrophages, epithelioid cells (ECs), multinucleated giant cells (MGCs), surrounded by a rim of T lymphocytes [3]. The organization and the cellular constituents of the developing *M. leprae* granulomas vary with the status of the host immune response. Presumptively, granulomatous lesions can be categorized within two polar forms [4]. At one extreme, tuberculoid granulomas are organized as nodular lesions with ECs and MGCs in the lesion center surrounded by a rim of fibrous connective tissue, lymphocytes along the periphery of the granuloma, and acid-fast bacilli are rarely demonstrable in the lesions. At the other extreme, the pathological feature of lepromatous leprosy skin lesions are characterized by a lack of organization of cells, with very high numbers of foamy macrophages containing very large numbers of bacilli, and disorganized lymphocyte infiltration.

* Correspondence: yumi@nih.go.jp

²Department of Mycobacteriology, Leprosy Research Center, National Institute of Infectious Diseases, 4-2-1 Aobacho, Higashimurayama, Tokyo 189-0002, Japan

Full list of author information is available at the end of the article

Granulomas have long been believed to benefit the host by containing and restricting the growth of mycobacteria in a localized area, to prevent the spread of the disease to other parts of the tissue or organs [5]. However, some studies in zebra fish infected with *M. marinum* and *M. tuberculosis* suggested that the granulomas contribute to early bacterial growth and expanding infection [6-10].

The structure, function, and evolution of granulomas have been studied using various animal models [11,12], high-resolution chest computed tomography scans of pulmonary tuberculosis patients [13], and explanted tissues [5,14]. Interestingly, the *in vitro* models of human mycobacterial granulomas have been studied by infection with Bacillus Calmette-Guérin (BCG) or stimulation with antigens such as purified protein derivatives or artificial beads coated with mycobacterial components [15,16]. These studies have identified infected macrophages, ECs, and several types of MGCs, which are thought to play important roles in the formation and maintenance of granulomas. In addition, macrophages demonstrate considerable plasticity that allows them to efficiently respond to environmental signals. These cells are generally classified as M1 (classic) macrophages, which produce proinflammatory cytokines and mediate resistance to pathogens and contribute to tissue destruction, or M2 (alternative) macrophages, that produce anti-inflammatory cytokines and promote tissue repair [17-19]. However, so far, we know little about the relationship between the polarization of macrophages within mycobacterial granulomas.

In this study, we developed an *in vitro* model of *M. leprae* granulomas, which mimicked the human granulomatous skin lesion with progressive recruitment of monocytes around macrophages infected by *M. leprae*, and their differentiation into ECs and MGCs as well as recruitment of activated lymphocytes. This model may be useful for unravelling the mechanisms of disease progression, and find effective strategies to control the spread of bacilli.

Methods

Ethics statement, cell culture and preparation of the bacteria

Peripheral blood was obtained from healthy Japanese individuals with informed consent. The study was approved by the ethics committee of the National Institute of Infectious Diseases (NIID). In Japan, BCG vaccination is compulsory for children aged 0–4 years old. Macrophages were differentiated from monocytes using granulocyte-macrophage colony-stimulating factor (GM-CSF) as described previously [20,21]. Animal experiments were carried out in strict accordance with the recommendations of Japan's Animal Protection Law. The protocol was approved by the Experimental Animal Committee of NIID Tokyo (Permit

Number: 211002). *M. leprae* (Thai-53 strain) was propagated in athymic BALB/c-*nu/nu* mice (Clea Co, Tokyo) [22]. At 8–9 months post-infection, mouse footpads were processed to recover *M. leprae* [23]. For all experiments, *M. leprae* was freshly prepared. Human cells without the bacilli were cultured at 37°C but when infected with the bacilli, the cells were cultured at 35°C to maintain the viability of *M. leprae* in host cells.

Culture of macrophages and peripheral blood mononuclear cells for the formation of cellular aggregates

Macrophages, differentiated from monocytes using GM-CSF after 4 days culture in RPMI containing 20% fetal calf serum (FCS) were transferred into 24-well tissue culture plates (Falcon) ($1 \sim 2 \times 10^5$ cells/well). Freshly prepared *M. leprae* were then added to each well. The multiplicity of infection (MOI: 50) was determined based on the assumption that macrophage were equally susceptible to infection with *M. leprae* [24]. After 24 hr, autologous peripheral blood mononuclear cells (PBMCs) were cultured with *M. leprae* infected macrophages at a ratio of 5:1 (PBMCs: macrophages). In some cases, macrophages were infected with *M. leprae* without PBMCs and in others, macrophages and PBMCs were co-cultured and macrophages alone were used as negative controls. The cells were cultured at 35°C for periods from 24 h to 10 days with medium changes every other day. To detach the cells from plates TrypLE Express (Gibco) was used, and then the cells were maintained in medium containing 10%FCS for 30 min, before processing for flow cytometric analyses. In other experiments we have also isolated T lymphocytes and monocytes were isolated using Dynabeads Untouched Human T cells and Dynabeads MyPure Monocyte kit 2 (Invitrogen), and used instead of PBMCs.

Phase-contrast microscopy and fluorescence microscopy

Macrophages grown on a 13-mm coverslip in a 24-well plate, were infected with *M. leprae* for 24 h. Autologous PBMCs were then co-cultured with macrophages for additional 9 days. Macrophages were fixed in 2% paraformaldehyde, or methanol pre-chilled to -20°C , and then observed under a phase-contrast microscope (Olympus CKX41 with $\times 10$ and $\times 20$ objective lenses). Photographs were taken with an Olympus DP50 system. Image acquisition and data processing were performed using DP controller software. In other experiments, cells were stained with May-Grünwald-Giemsa stain (MGG) (Sigma-Aldrich) or by TB Carbofuchsin ZN stain according to the manufacturer's instructions (BD Biosciences).

Cell imaging was performed using LSM5-Exciter laser scanning microscope equipped with a 568 nm laser (Carl Zeiss). Fixed cells were stained with anti-human CD163 monoclonal antibody (mAb: BioLegend) and the

secondary antibody used was an Alexa Fluor 568-conjugated goat anti-mouse IgG (Invitrogen/Molecular Probes). Nuclei were counterstained with Hoechst 33342 dye (Sigma-Aldrich). *M. leprae* was stained by auramine O (BD Biosciences). Images were obtained under a fluorescence confocal microscope. Data were processed using LSM software ZEN 2007.

Analysis of cell surface antigens on macrophages by flow cytometry and microscopy

Macrophages were collected after time points of 1 and 9 days of co-culture with the PBMCs or *M. leprae* stimulation. The expression of cell surface antigens on macrophages, was analyzed using a FACSCalibur flow cytometer (BD Biosciences). Dead cells were eliminated from the analysis by staining with 7-amino actinomycin D. For the analysis of cell surface antigens, the following mAb were used: FITC-conjugated mAb against CD68 (KP) was purchased from Dako, FITC conjugated TLR4 (HTA125) and CD206 (19.2), and PE conjugated mAb against CD86 (FUN-1) was all purchased from BD Biosciences and PE conjugated mAb to CD14 (HCD14) and CD163 (RM3/1) were from BioLegend. The numbers in the insets indicate the mean fluorescent values of the cells stained with the respective mAbs.

Determination of cytokine levels

The levels of the cytokines: Interferon (IFN)- γ , interleukin (IL)-2, tumor necrosis factor (TNF)- α , IL-12p40, IL-1 β and IL-10 in the culture supernatants were quantified using enzyme assay kits, OptEIA Human ELISA Set (BD Biosciences) and processed according to the manufacturer's instructions. IL-4 and IL-13 was purchased from MABTECH AB. Cytokine levels were expressed as pg of protein/ml of protein. Real-time PCR analysis of mRNA extracted using an RNeasy Mini kit (Qiagen), was performed using SYBR Green PCR Master Mix (Applied Biosystems) with specific primers according to the manufacturer's instructions. The instrument used for the detection of the expression of mRNA was StepOnePlus with StepOne software.

Determination of *M. leprae* viability

The viability of *M. leprae* recovered from the macrophages of different groups was detected by radiorespirometry, that measures the oxidation of ^{14}C palmitic acid to $^{14}\text{CO}_2$, as described previously [25]. Briefly, the adherent macrophages and granulomas with bacilli were lysed in 300 μl of a 0.1 N NaOH solution to release intracellular *M. leprae*. After neutralization with 0.1 N HCl solution, an equal volume of 2 times concentrated Middlebrook 7H9 broth was added. ^{14}C labeled palmitic acid was added to the lysates of macrophages or granulomas, followed by incubation at 33°C. After 7 days, cumulative amounts of oxidized palmitic

acid released as $^{14}\text{CO}_2$ by metabolically active *M. leprae* were measured using a Packard 1500 TRI-CARB liquid scintillation analyzer. The unpaired Student's t-test was used to determine the statistical significance of the two data sets.

Results

Granuloma-like aggregates formed by co-culture of *M. leprae* infected macrophages and autologous PBMCs

When PBMCs were incubated with *M. leprae* infected macrophages in a 24-well tissue culture plate, the cells aggregated to form a multilayered granuloma-like aggregates by day 9 as shown in Figure 1A, whereas control groups did not recruit any cells at this stage (Figure 1B, C). We observed formation of a granular ball-like structure caused by some synapses around aggregates. These *in vitro* granulomas exhibited a cellular structure similar to that in histopathological specimens of tuberculoid leprosy lesions showing T lymphocytes surrounding the differentiated, ECs and MGCs that may be involved in cytokine production for intercellular communication. (Figure 1D). Confocal microscopic analysis of *M. leprae*-induced granuloma showed a multilayered structure (about 3–4 cell layers in transverse and straight sections), and some cells were positive for CD163 (red), a macrophage marker (Figure 1E).

Characterization of the cell populations recruited within *in vitro* granuloma-like aggregates

To identify and characterize the different cell types in granuloma-like aggregates, the cells were plated on glass slides and stained on day 9 of co-culture. MGG staining showed that activated macrophages with larger cytoplasm, and MGCs were observed, which resembled those in the granulomas of leprosy (Figure 2B, D). MGCs are thought to be formed as a result of fusion of macrophages, monocytes and ECs (Figures 2A, C). The presence of *M. leprae* in MGCs was confirmed by staining with TB Carbol-fuchsin ZN (arrows in Figure 2E, F). In addition, confocal microscopy revealed the presence of MGCs with auramine O stained *M. leprae*, in the cytoplasmic region (Figure 2G, H). To characterize macrophages, ECs and MGCs in the granuloma-like aggregates, we performed immunofluorescence staining for macrophage markers CD68, CD1a and CD163 (data not shown). Both the macrophages and the MGCs could express the CD68 and CD1a marker, but the expression level of CD68 on the macrophages was higher than that on the MGCs. With the increasing number of nuclei in MGCs, lower levels of CD68 was observed (not shown), although there was no significant difference in the expression levels of CD1a between macrophages and MGCs. These data indicate that MGCs belong to the monocyte/macrophage lineage.

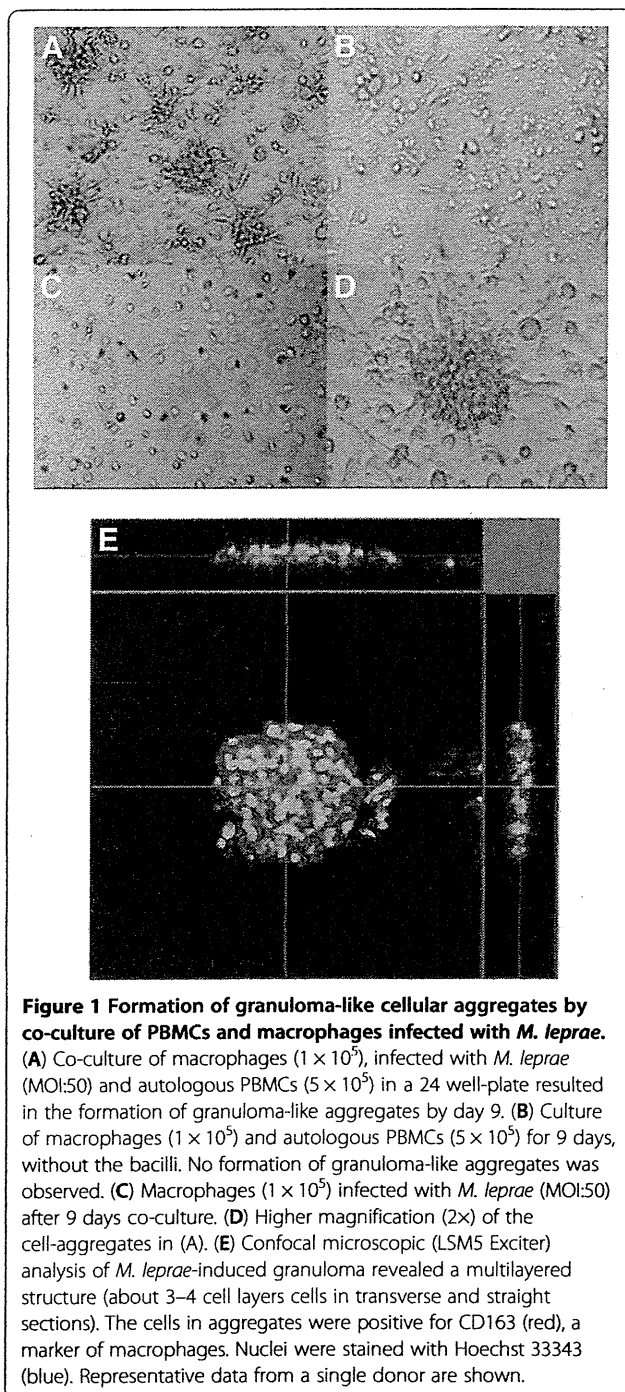


Figure 1 Formation of granuloma-like cellular aggregates by co-culture of PBMCs and macrophages infected with *M. leprae*. (A) Co-culture of macrophages (1×10^5), infected with *M. leprae* (MOI:50) and autologous PBMCs (5×10^5) in a 24 well-plate resulted in the formation of granuloma-like aggregates by day 9. (B) Culture of macrophages (1×10^5) and autologous PBMCs (5×10^5) for 9 days, without the bacilli. No formation of granuloma-like aggregates was observed. (C) Macrophages (1×10^5) infected with *M. leprae* (MOI:50) after 9 days co-culture. (D) Higher magnification (2x) of the cell-aggregates in (A). (E) Confocal microscopic (LSM5 Exciter) analysis of *M. leprae*-induced granuloma revealed a multilayered structure (about 3–4 cell layers cells in transverse and straight sections). The cells in aggregates were positive for CD163 (red), a marker of macrophages. Nuclei were stained with Hoechst 33343 (blue). Representative data from a single donor are shown.

Expression levels of cell surface antigens on macrophages at different time points

We investigated the expression levels of cell surface antigens on macrophages from different groups at two different time points, day 1 and day 9. On day 1, there was no significant difference in the expression of cell surface antigens on macrophages between groups. Compared with day 1 macrophages, day 9 macrophages, which were infected with *M. leprae* and co-cultured with PBMCs to

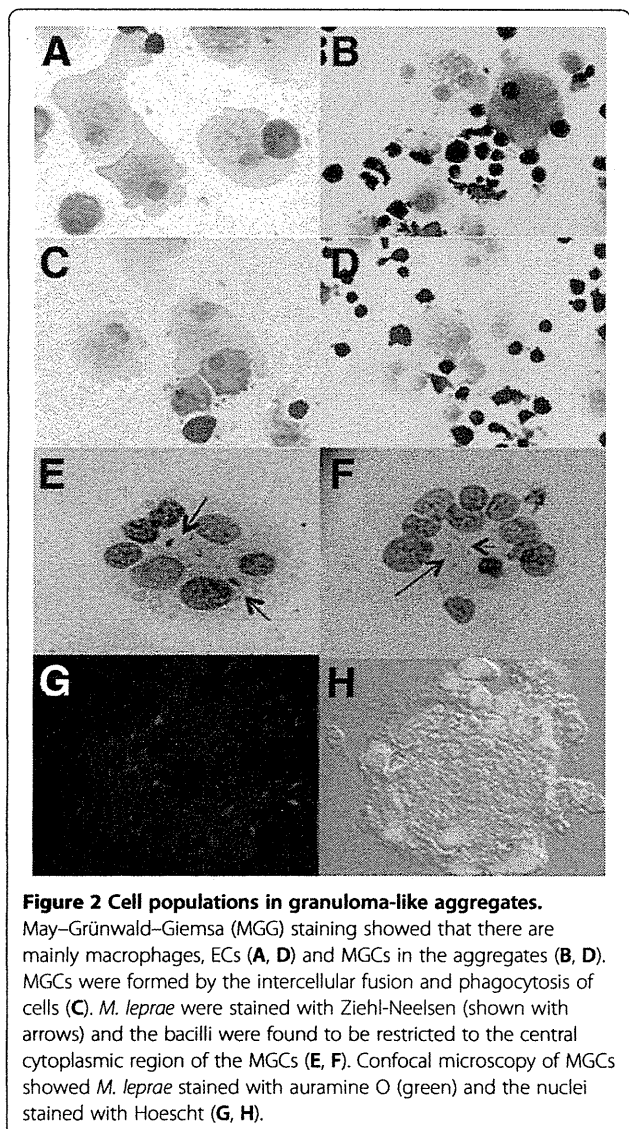


Figure 2 Cell populations in granuloma-like aggregates. May-Grünwald-Giemsa (MGG) staining showed that there are mainly macrophages, ECs (A, D) and MGCs in the aggregates (B, D). MGCs were formed by the intercellular fusion and phagocytosis of cells (C). *M. leprae* were stained with Ziehl-Neelsen (shown with arrows) and the bacilli were found to be restricted to the central cytoplasmic region of the MGCs (E, F). Confocal microscopy of MGCs showed *M. leprae* stained with auramine O (green) and the nuclei stained with Hoescht (G, H).

form granuloma-like aggregates, showed higher expression of CD14 (pattern recognition receptor), CD68 (macrophage marker related to phagocytic activities), CD163 (scavenger receptor) and CD206 (mannose receptor), although the expression of major histocompatibility complex (MHC) class-II, CD86, and toll-like receptor (TLR)-4 did not change (Figure 3). Interestingly, in our long-term culture (9 days) of macrophages infected with *M. leprae*, the expression of CD14, CD68, CD163, TLR4, CD86 and CD206 was significantly lower than that in macrophages infected with *M. leprae* and co-cultured with PBMCs. CD206 expression was the lowest in macrophages co-cultured with PBMCs, although CD163 expression was significantly high (Figure 3). CD163 and CD206 are markers of M2 macrophages, whereas CD86 expression is associated with M1 macrophages. Therefore, the M1 and M2 macrophages appeared to coexist in granulomas.

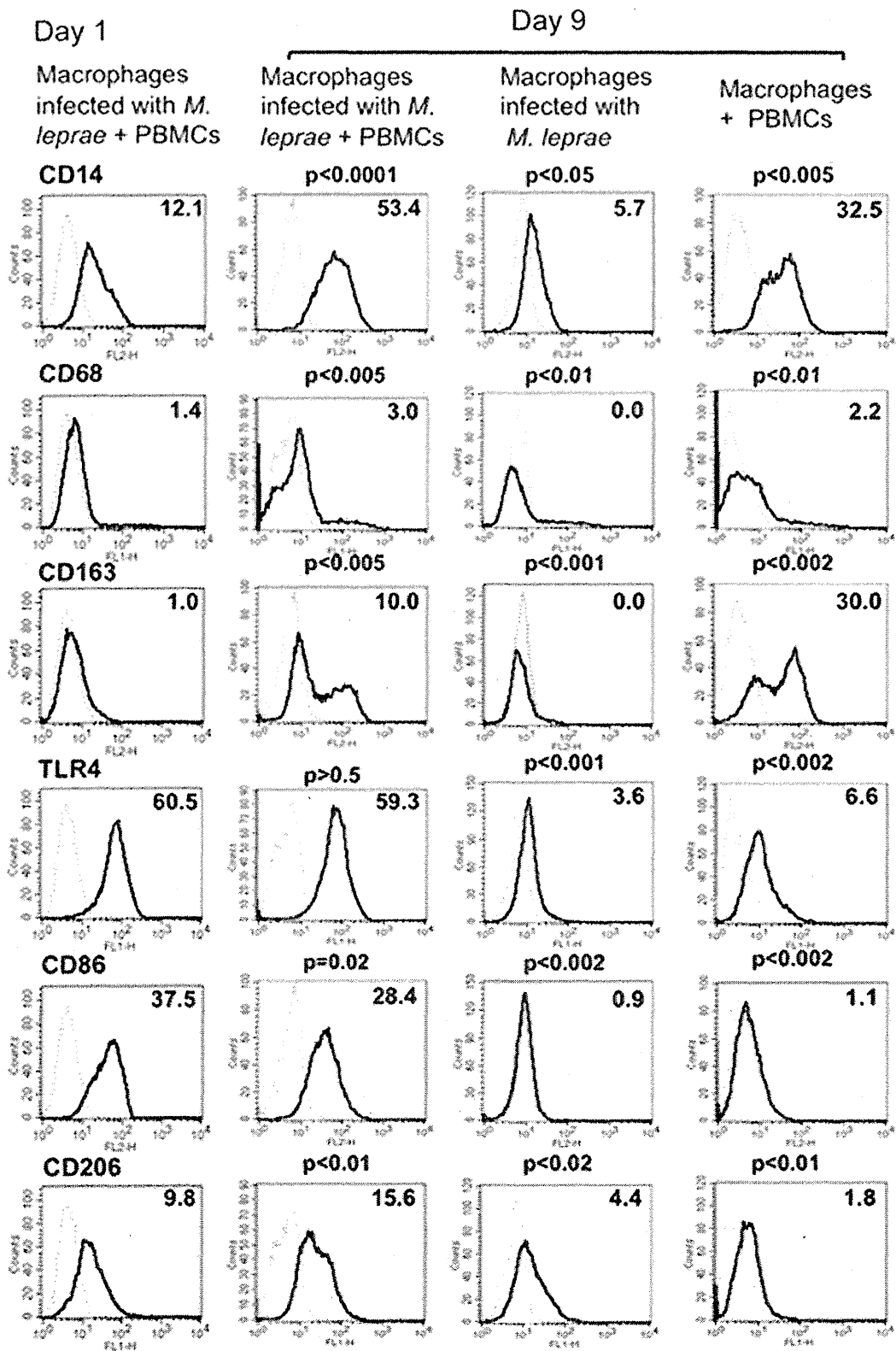


Figure 3 (See legend on next page.)

(See figure on previous page.)

Figure 3 Expression of cell surface antigens on macrophages at two different time points. Compared with the control group on day 1, day 9 macrophages infected with *M. leprae* and co-cultured with T lymphocytes showed relatively higher expression of CD14, CD163 and CD206. While in macrophages infected with *M. leprae*, the expression level of CD14, CD68, CD163, TLR4, CD86 and CD206, were downregulated as compared to those infected macrophages co-cultured with PBMCs. Representative data of one donor, from three independent experiments are shown. P-values were calculated using the Welch unpaired t-test in comparison with day 1 macrophages.

Cytokines in culture supernatants

The culture supernatants from different groups were collected on days 1, 3 and 9 after the start of macrophage culture. The release of IFN- γ , IL-2, TNF- α , IL-12p40, IL-1 β , IL-4 and IL-13, was evaluated by ELISA (Figure 4). Interestingly, the expression levels of the various cytokines in supernatants, from different groups showed significant differences that were associated with the formation of granuloma-like aggregates and changes of cell surface antigen expression on macrophages. In the group with *M. leprae* infected macrophages co-cultured with PBMCs, the concentrations of IL-2, IL-1 β and TNF- α peaked on day 1 after infection and then declined gradually. The level of IL-12 p40 also declined slowly by day 9. IFN- γ levels were low on day 1, but increased 7 fold by day 4, and then remained unchanged till day 9. A high level of IL-10 expression in macrophages and macrophages cultured with PBMCs was observed, but the expression was significantly decreased when macrophages were infected with *M. leprae* as observed in the day 9 cytokine expression levels. However,

when macrophages were differentiated with M-CSF, the expression of IL-10 was significantly high when macrophages were infected with *M. leprae* (Additional file 1: Figure S1). IL-4 and IL-13 were not detected in any groups on days 1 and 9 from the start of macrophage culture (data not shown). Real time PCR results further confirmed the cytokine expression and showed similar results except for the IL-2 and TNF- α , whose expression was observed in control groups of macrophages infected with *M. leprae* in addition to those co-cultured with PBMCs (Figure 5).

The viability of *M. leprae* in granuloma-like aggregates

We determined the viability of *M. leprae* at days 1 and 9, when granuloma-like aggregates were observed in co-cultures of *M. leprae* infected macrophages with PBMCs, whereas in cultures of macrophages infected with *M. leprae*, there was no granuloma formation. The amount of radioactive CO₂ evolved which reflects the rate of ¹⁴C-palmitic acid oxidized by *M. leprae*, which was measured by a scintillation counter. No significant difference in ¹⁴CO₂

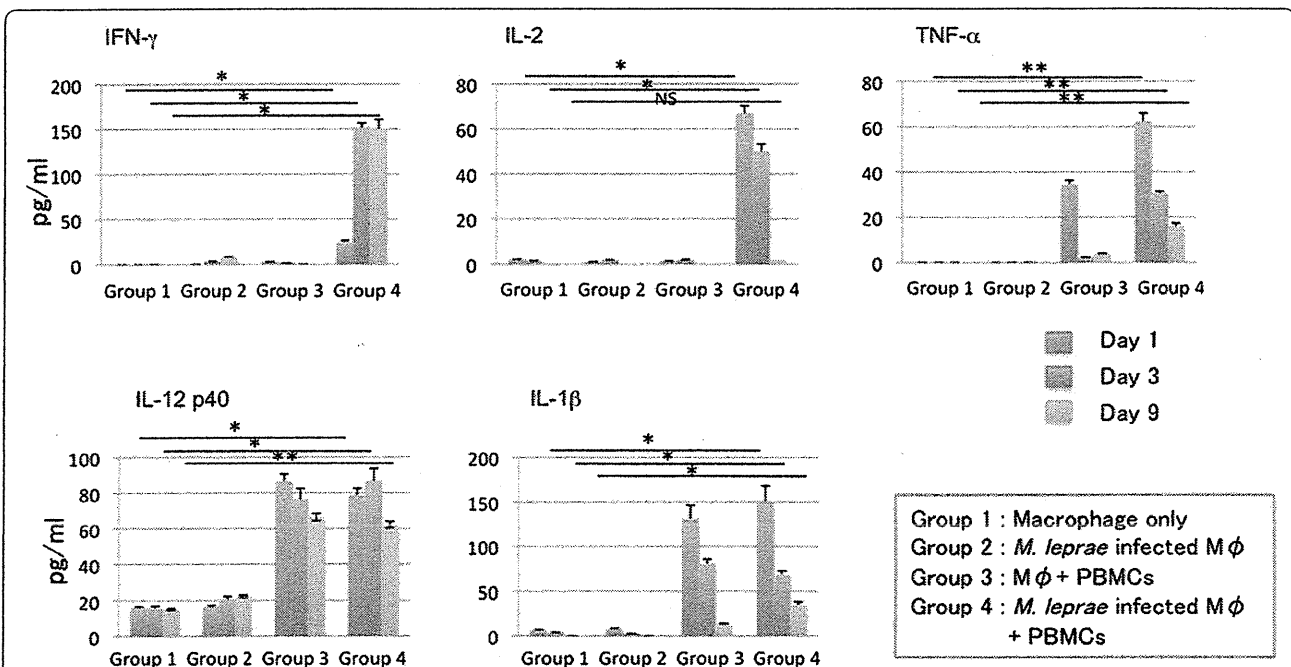
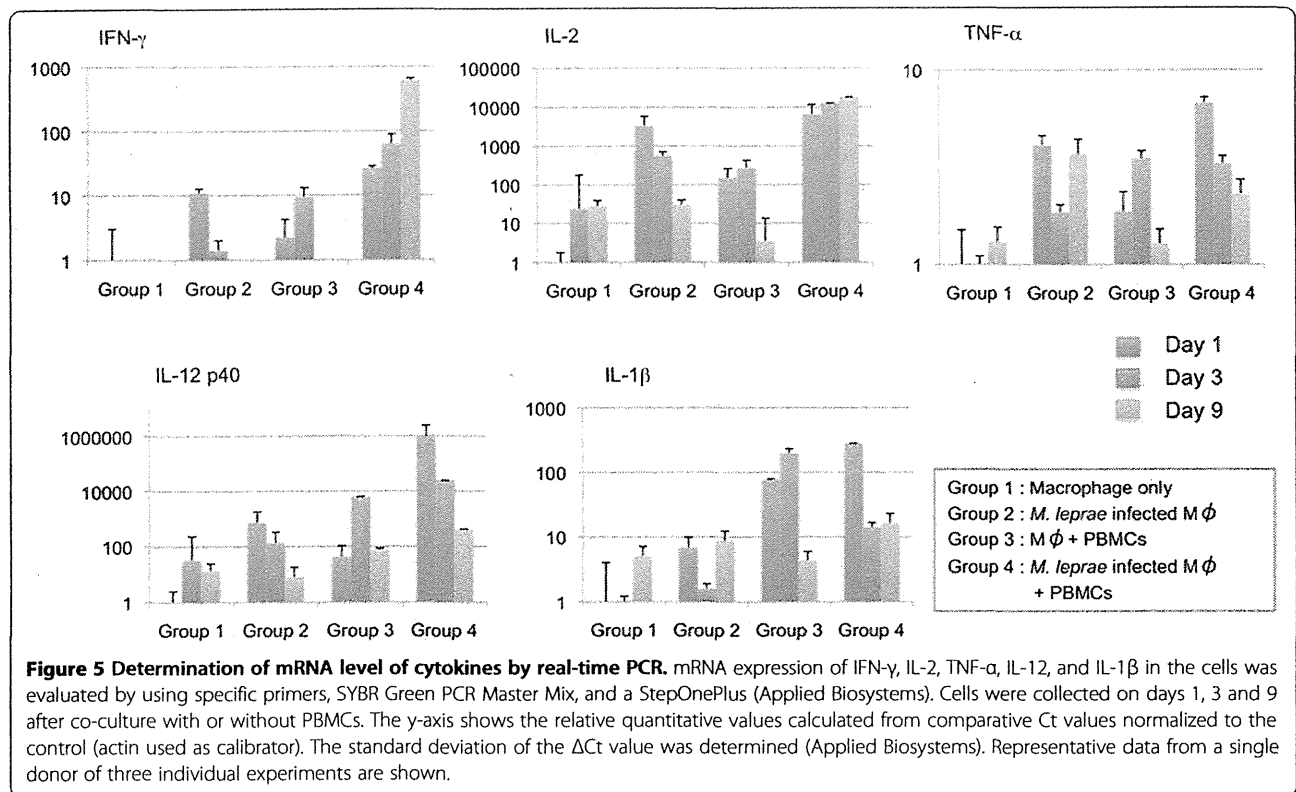


Figure 4 Measurement of cytokines secreted into the culture medium by ELISA. Measurement of IFN- γ , IL-2, TNF- α , IL-12, and IL-1 β secreted in the culture medium from different groups of cells at day 1, 3 and 9. Representative data from three individual experiments of a single donor are shown. Unpaired Student's t-test was performed. NS: not significant, *p < 0.001, **p < 0.01.



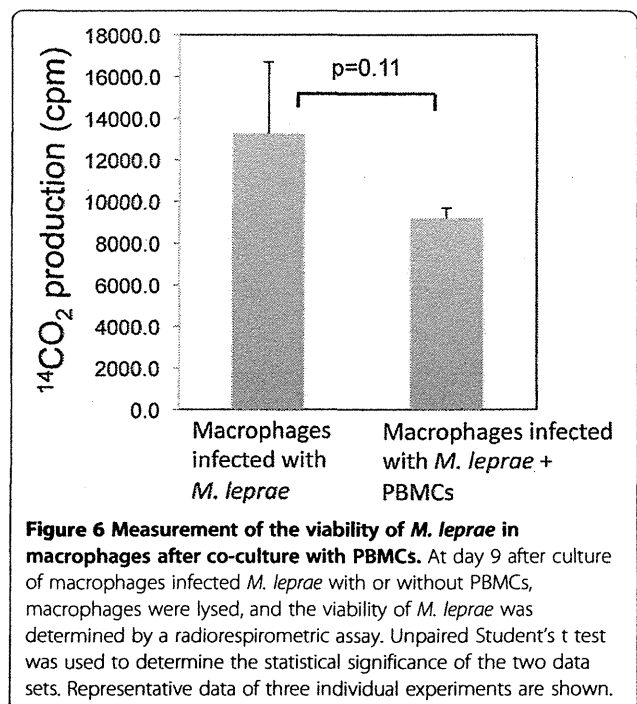
production was observed from macrophage in either groups on days 1, and 9. However, the amount of radioactive CO₂ released from macrophages infected with *M. leprae* and co-cultured with PBMCs for 9 days was lower but not significantly lower than that released from macrophages infected with *M. leprae* alone (Figure 6).

Discussion

In the 1960s, Ridley and Jopling proposed a histological classification scheme for leprosy [26]. At one extreme, called the polar tuberculoid, leprosy patients show a high degree of cell-mediated immunity, lesions revealing well-developed granulomatous inflammation and rarely acid-fast bacilli are detected. At the other extreme, termed polar lepromatous patients have no apparent resistance to *M. leprae*, and skin biopsies reveal sheets of foamy macrophages in the dermis containing very large numbers of bacilli and microcolonies called globi. Currently, the formation and maintenance of granulomas are considered to be critical components of the host response to *M. leprae* infection, which determine not only whether primary disease occurs, but also the clinical manifestation. Granuloma formation is studied in mouse models but little is known about the human granuloma due to the ethical problems of using human samples and the difficulties in establishing a good model using human cell lines.

The formation of small, rounded granuloma-like-structure, was previously described by co-culture of blood lymphocytes

with autologous macrophages infected with *M. tuberculosis*, or BCG or stimulation with other mycobacterial antigen such as purified protein derivatives. These granuloma-like structures showed abundance of CD68 positive macrophages with small round lymphocytes scattered throughout the



granuloma [15,16]. These models not only exhibit structural similarities to granulomas observed in human clinical specimens, but also show patterns of cell antigen expression and/or cytokine production that appear consistent with those observed in tuberculosis patients. However, the formation of granulomas in leprosy, involving *M. leprae* infection has not been previously studied *in vitro*. The only data available on granuloma formation of leprosy is from the immunological staining of biopsies of patients, and granulomas harvested from the footpads of athymic nude mice [27].

In our model, we first infected the immature human macrophages with *M. leprae*. To mimic the recruitment of additional PBMCs which would occur *in vivo*, autologous PBMCs were added after 24 h and cultured at 35°C, the optimal temperature for the growth of *M. leprae* and macrophages to be kept viable. Within 9 days of culture, macrophages and T lymphocytes gathered to form a granuloma-like aggregates with fused macrophages, appearing as multinucleated cells, and epithelioid macrophages tightly linked to surrounding macrophages and lymphocytes. However, in control groups, the formation of granuloma-like aggregates was not observed. When autologous T lymphocytes and monocytes were purified and used instead of PBMCs, a similar formation of granuloma like aggregates were observed, together with production of the same amounts of cytokines, indicating that T lymphocytes and monocytes are sufficient for the containment of *M. leprae* in granuloma like structures.

Electron microscopy studies indicated that the tuberculoid lesion had an appearance of a granulomatous response with a predominance of ECs and MGCs, and the mononuclear phagocytes which are surrounded by a mantle of lymphocytes [28]. In the present *in vitro* model of granulomas, MGCs were prominent, and resembled MGCs observed in a tuberculoid lesion. MGCs have been described by Langhans, but the function of these cells in the granuloma remains to be elucidated [29]. In this study, we observed not only Langhans giant cells (MGCs with a circular nuclear organization in contrast to the MGCs formed in response to a foreign body that lacks this kind of organization), but also the bacilli surrounded by nuclei and restricted to the central cytoplasmic region. Because this type of MGC is not observed in the normal mouse model, it is interesting to further focus on the formation, mechanism and function of such MGCs using human *in vitro* model or humanized mouse model as recently described by Heuts et al. [30]. The *in vitro* model of leprosy granulomas still needs to be investigated, and compared to that obtained using leprosy patients' monocytes and T cells.

Macrophages function as control switches of the immune system, providing a balance between pro- and anti-inflammatory responses by developing into subsets of M1 or M2 activated macrophages. M1 macrophages

are activated by type I cytokines such as IFN- γ and TNF α . Alternatively, activated M2 macrophages are subdivided further into M2a (activated by IL-4 or IL-13), M2b (activated by immune complexes in combination with IL-1 β) and M2c (activated by IL-10 or glucocorticoids) [31]. M1 macrophages exhibit a potent microbicidal activity, and release IL-12, promoting strong Th1 immune responses. It is the M1 population that is thought to contribute to macrophage-mediated tissue injury [19,32]. In contrast, M2 macrophages support Th2-associated effector functions and exert a selective immunosuppressive activity. M2 macrophages also play a role in the resolution of inflammation through phagocytosis of apoptotic neutrophils, reduced production of pro-inflammatory cytokines, and increased synthesis of mediators that are important for tissue remodeling and wound repair. We investigated the contribution of the macrophage polarization, MGC formation and immune responses against *M. leprae* in granulomas, and found that there was a strong relationship between the formation of granuloma-like aggregates, the changes of cell surface antigen expression on macrophages, and the expression levels of various cytokines with the macrophage polarization. In *M. leprae* infected macrophages cocultured with PBMCs, the concentrations of IL-2, IL-12 and TNF- α peaked at day 1, while, TLR4, CD86, and MHC molecules were highly expressed, indicating that most of the macrophages were of the M1 subset. At day 9, in the same group of infected macrophages cocultured with PBMCs, the cells assembled and formed a multilayer, granuloma-like aggregates, and the macrophages not only highly expressed TLR4 and CD86, but also scavenger receptor (CD163) and mannose receptor (CD206) molecules. CD163 and CD206 are the markers of M2 macrophages. Therefore, the M1 and M2 macrophages coexisted in granuloma-like aggregates. Consistent with this observation, the levels of IL-1 β , IL-2, IL-12 and IFN- γ were high in the culture medium, promoting the differentiation of macrophages into both M1 and M2 subsets. The protective cell mediated immune response is regulated by the cytokine equilibrium, while the tuberculoid pole is characterized by the presence of Th1 cytokines (IL-2, IFN- γ , TNF- α and IL-12), and lepromatous is characterized by type 2 cytokines (IL-4, IL-6 and IL-10) [33]. Because IL-10 is an immunosuppressive cytokine implicated in susceptibility to mycobacterial infection, we examined the expression of IL-10 in more detail. Indeed, the infection with *M. leprae* suppressed the production of IL-10. However, when macrophages were differentiated with M-CSF, rather than GM-CSF, *M. leprae* infection further enhanced IL-10 production. Our results indicate that the granuloma aggregates studied here, are similar to those observed in the tuberculoid form of leprosy. However, little is known about the type

of cytokines that influence the formation of macrophages for containment of *M. leprae* in the granulomas during the pathogenesis of leprosy.

We also investigated the viability of *M. leprae* in macrophages at different time points. At day 9, a number of granuloma-like aggregates were observed in co-cultures of PBMCs with macrophages infected with *M. leprae*. However in macrophages infected with *M. leprae* without the PBMCs, granuloma-like aggregates were not observed. There were no significant differences in the viability of *M. leprae* in macrophage of different groups on day 1, but on day 9, the viability of *M. leprae* in the group that formed granuloma-like aggregates was slightly lower, although not significantly, than that of *M. leprae* in infected macrophages without PBMCs. Evidently, granuloma-like aggregates appear to benefit the host but the bacilli remained metabolically active. The mechanism of this phenomenon needs further in-depth analysis.

Conclusions

In summary, we have developed for the first time a method to obtain *in vitro* *M. leprae* granulomas using human monocyte derived macrophages and PBMCs. Using this model, we obtained some basic information about the characteristics of *in vitro* granulomas. In addition, the viability of *M. leprae* in granuloma-like aggregates remained unaltered during the culture period. Effective strategies to allow the bacilli to succumb to the formation of granuloma may assist in the primary control of the infection.

Additional file

Additional file 1: Figure S1. Measurement of IL-10 secreted into the culture medium by ELISA. Measurement of IL-10 secreted in the culture medium from different groups of cells at days 2, 6 and 9 is shown. Two types of macrophages were used to analyze the data. (A) Macrophages differentiated using GM-CSF, and (B) macrophages differentiated from monocytes using M-CSF. Representative data from two individual experiments of a single donor are shown. Unpaired student's t test was performed, * $p < 0.0001$, ** $p < 0.001$, *** $p < 0.05$.

Abbreviations

DCs: Dendritic cells; PBMCs: Peripheral blood mononuclear cells; ECs: Epitheloid cells; MGCs: Multinucleated giant cells; BCG: Bacillus Calmette- Guérin.

Competing interests

The authors declare that they have no competing interests.

Authors' contributions

HW, YM participated in the design of the study and carried out the cell culture experiments, YF carried out the confocal microscopic examination, and radio-respirometric assay. HW, YM, and MM were involved in the preparation of the manuscript. All authors have read and approved the final manuscript.

Acknowledgments

This study was supported by grants from the Grant-in-Aid from the Ministry of Health, Labor and Welfare of Japan for "Research on Emerging and Re-emerging Infectious Diseases" (Grant no. H24-Shinko-Ippan-009 to YM)

and also from the National Natural Science Foundation of China (30972651), the fund for Key Clinical Program of the Ministry of Health (2010-2012-125). We appreciate the helpful assistance of Drs. Masanori Matsuoka and Masanori Kai for the *M. leprae* propagation and isolation. We also thank the Japanese Red Cross Society for kindly providing whole blood cells from healthy donors.

Author details

¹Institute of Dermatology, Chinese Academy of Medical Sciences and Peking Union Medical College, 12 Jiangwangmiao Road, Nanjing 210042, China.

²Department of Mycobacteriology, Leprosy Research Center, National Institute of Infectious Diseases, 4-2-1 Aobacho, Higashimurayama, Tokyo 189-0002, Japan.

Received: 13 December 2012 Accepted: 17 June 2013

Published: 20 June 2013

References

1. Britton WJ: Immunology of leprosy. *Trans R Soc Trop Med Hyg* 1993, **87**:508-514.
2. Kaplan G, Cohn ZA: The immunobiology of leprosy. *Int Rev Exp Pathol* 1986, **28**:45-78.
3. Saunders BM, Cooper AM: Restraining mycobacteria: role of granulomas in mycobacterial infections. *Immunol Cell Biol* 2000, **78**:334-341.
4. Rojas-Espinosa O, Løvik M: *Mycobacterium leprae* and *Mycobacterium lepraemurium* infections in domestic and wild animals. *Rev Sci Tech* 2001, **20**:219-251.
5. Ulrichs T, Kaufmann SH: New insights into the function of granulomas in human tuberculosis. *J Pathol* 2006, **208**:261-269.
6. Clay H, Volkman HE, Ramakrishnan L: Tumor necrosis factor signaling mediates resistance to mycobacteria by inhibiting bacterial growth and macrophage death. *Immunity* 2008, **29**:283-294.
7. Dannenberg AM Jr: Immunopathogenesis of pulmonary tuberculosis. *Hosp Pract (Off Ed)* 1993, **28**(1):51-58.
8. Lesley R, Ramakrishnan L: Insights into early mycobacterial pathogenesis from the zebrafish. *Curr Opin Microbiol* 2008, **11**:277-283.
9. Tobin DM, Ramakrishnan L: Comparative pathogenesis of *Mycobacterium marinum* and *Mycobacterium tuberculosis*. *Cell Microbiol* 2008, **10**:1027-1039.
10. Davis JM, Ramakrishnan L: The role of the granuloma in expansion and dissemination of early tuberculous infection. *Cell* 2009, **136**:37-49.
11. Bouley DM, Ghori N, Mercer KL, Falkow S, Ramakrishnan L: Dynamic nature of host-pathogen interactions in *Mycobacterium marinum* granulomas. *Infect Immun* 2001, **69**:7820-7831.
12. Saunders BM, Frank AA, Orme IM, Cooper AM: CD4 is required for the development of a protective granulomatous response to pulmonary tuberculosis. *Cell Immunol* 2002, **216**:65-72.
13. Poey C, Verhaegen F, Giron J, Lavayssiere J, Fajadet P, Duparc B: High resolution chest CT in tuberculosis: evolutive patterns and signs of activity. *J Comput Assist Tomogr* 1997, **21**:601-607.
14. Tsai MC, Chakravarty S, Zhu G, Xu J, Tanaka K, Koch C, Tufariello J, Flynn J, Chan J: Characterization of the tuberculous granuloma in murine and human lungs: cellular composition and relative tissue oxygen tension. *Cell Microbiol* 2006, **8**:218-232.
15. Puissegur MP, Botanch C, Duteyrat JL, Delsol G, Caratero C, Altare F: An *in vitro* dual model of mycobacterial granulomas to investigate the molecular interactions between mycobacteria and human host cells. *Cell Microbiol* 2004, **6**:423-433.
16. Birkness KA, Guarner J, Sable SB, Tripp RA, Kellar KL, Bartlett J, Quinn FD: An *in vitro* model of the leukocyte interactions associated with granuloma formation in *Mycobacterium tuberculosis* infection. *Immunol Cell Biol* 2007, **5**:160-168.
17. Krausgruber T, Blazek K, Smallie T, Alzabin S, Lockstone H, Sahgal N, Hussell T, Feldmann M, Udalova IA: IRF5 promotes inflammatory macrophage polarization and TH1-TH17 responses. *Nat Immunol* 2011, **12**:231-238.
18. Satoh T, Takeuchi O, Vandenbon A, Yasuda K, Tanaka Y, Kumagai Y, Miyake T, Matsushita K, Okazaki T, Saitoh T, Honma K, Matsuyama T, Yui K, Tsujimura T, Standley DM, Nakanishi K, Nakai K, Akira S: The *Tmj3d3-Irf4* axis regulates M2 macrophage polarization and host responses against helminth infection. *Nat Immunol* 2010, **11**:936-944.

19. Benoit M, Desnues B, Mege JL: **Macrophage polarization in bacterial infections.** *J Immunol* 2008, **181**:3733–3739.
20. Makino M, Baba M: **A cryopreservation method of human peripheral blood mononuclear cells for efficient production of dendritic cells.** *Scand J Immunol* 1997, **45**:618–622.
21. Maeda Y, Mukai T, Spencer J, Makino M: **Identification of an immunomodulating agent from *Mycobacterium leprae*.** *Infect Immun* 2005, **73**:2744–2750.
22. Levy L, Ji B: **The mouse foot-pad technique for cultivation of *Mycobacterium leprae*.** *Lepr Rev* 2006, **77**:5–24.
23. McDermott-Lancaster RD, Ito T, Kohsaka K, Guelpa-Lauras CC, Grosset JH: **Multiplication of *Mycobacterium leprae* in the nude mouse, and some applications of nude mice to experimental leprosy.** *Int J Lepr Other Mycobact Dis* 1987, **55**:889–895.
24. Hashimoto K, Maeda Y, Kimura H, Suzuki K, Masuda A, Matsuoka M, Makino M: ***Mycobacterium leprae* infection in monocyte-derived dendritic cells and its influence on antigen-presenting function.** *Infect Immun* 2002, **70**:5167–5176.
25. Truman RW, Krahenbuhl JL: **Viable *Mycobacterium leprae* as a research reagent.** *Int J Lepr Other Mycobact Dis* 2001, **69**:1–12.
26. Ridley DS, Jopling WH: **Classification of leprosy according to immunity. A five-group system.** *Int J Lepr Other Mycobact Dis* 1966, **34**:255–273.
27. Hagge DA, Ray NA, Krahenbuhl JL, Adams LB: **An in vitro model for the lepromatous leprosy granuloma: Fate of *Mycobacterium leprae* from target macrophages after interaction with normal and activated effector macrophages.** *J Immunol* 2004, **172**:7771–7779.
28. Kaplan G, Van Voorhis WC, Sarno EN, Nogueira N, Cohn ZA: **The cutaneous infiltrates of leprosy. A transmission electron microscopy study.** *J Exp Med* 1983, **158**:1145–1159.
29. Postlethwaite AE, Jackson BK, Beachey EH, Kang AH: **Formation of multinucleated giant cells from human monocyte precursors. Mediation by a soluble protein from antigen- and mitogen-stimulated lymphocytes.** *J Exp Med* 1982, **155**:168–178.
30. Heuts F, Gavier-Widen D, Carow B, Juarez J, Wigzell H, Rottenberg ME: **CD4+ cell dependent granuloma formation in humanized mice infected with mycobacteria.** *PNAS* 2013, **110**:6482–6487.
31. Laskin DL: **Macrophages and Inflammatory Mediators in Chemical Toxicity: A Battle of Forces.** *Chem Res Toxicol* 2009, **22**:1376–1385.
32. Trujillo G, O'Connor EC, Kunkel SL, Hogaboam CM: **A novel mechanism for CCR4 in the regulation of macrophage activation in bleomycin-induced pulmonary fibrosis.** *Am J Pathol* 2008, **172**:1209–1221.
33. Yamamura M, Wang XH, Ohmen JD, Uyemura K, Rea TH, Bloom BR, Modlin RL: **Cytokine patterns of immunologically mediated tissue damage.** *J Immunol* 1992, **149**:1470–1475.

doi:10.1186/1471-2334-13-279

Cite this article as: Wang et al.: An in vitro model of *Mycobacterium leprae* induced granuloma formation. *BMC Infectious Diseases* 2013 **13**:279.

Submit your next manuscript to BioMed Central and take full advantage of:

- Convenient online submission
- Thorough peer review
- No space constraints or color figure charges
- Immediate publication on acceptance
- Inclusion in PubMed, CAS, Scopus and Google Scholar
- Research which is freely available for redistribution

Submit your manuscript at
www.biomedcentral.com/submit



REVIEW ARTICLE

Laboratory procedures for the detection and identification of cutaneous non-tuberculous mycobacterial infections

Kazue NAKANAGA,¹ Yoshihiko HOSHINO,¹ Rie R. YOTSU,² Masahiko MAKINO,¹ Norihisa ISHII¹

¹Leprosy Research Center, National Institute of Infectious Diseases, and ²Department of Dermatology, National Center for Global Health and Medicine, Tokyo, Japan

ABSTRACT

There is evidence that the incidence of cutaneous non-tuberculous mycobacterial (NTM) infection is increasing worldwide. Novel culture methods and new analytical procedures have led to significant advancements in understanding the origin and progression of NTM infections. Differential identification of NTM isolates is important because culture characteristics and/or sensitivity to anti-mycobacterium drugs vary between different mycobacterial species. In this manuscript, we describe the latest diagnostic techniques for cutaneous NTM infection and show how these methodologies can be used for the diagnosis of Buruli ulcer in Japan.

Key words: 16S rRNA gene, Buruli ulcer, cutaneous infection, non-tuberculous mycobacterial infection, polymerase chain reaction, species identification.

INTRODUCTION

The basis for the increase in the number of cases of cutaneous non-tuberculous mycobacterial (NTM) infection is unknown. It has been attributed to an increase in the total number of these patients or to better detection and/or reporting methods.^{1–5} Insight into the origin and progression of NTM infections has been significantly advanced due to the employment of novel methods for the culture and analysis of NTM. However, the diagnosis of a cutaneous NTM infection in less experienced hospitals is occasionally delayed, or not made at all, because the causative agent can be difficult to isolate due to its variety of growth characteristics. To date, most cutaneous NTM infections have been caused by *Mycobacterium marinum*^{6,7} or by groups of rapidly growing mycobacterial (RGM) species, but sometimes a rare mycobacterium can cause the disease.^{8–10} Different strains of mycobacteria generally exhibit different characteristics in culture and/or sensitivity to anti-mycobacterial drugs. Therefore, accurate identification of the causative agent is important for the treatment of NTM infections. In this manuscript, we describe the latest molecular diagnostic techniques for cutaneous NTM infection and present a case study that used these methodologies for BU diagnosis.

NTM IN DERMATOLOGY

Causative agents of dermatological infections

Approximately 30 mycobacterial species have been identified as causative agents of cutaneous infection (Table 1). These

species of mycobacteria, with the exception of the *Mycobacterium tuberculosis* complex and *Mycobacterium leprae*, are classified as NTM. They are categorized into four groups based on their growth rate (slow growing mycobacterial [SGM] and RGM species) and photochromogenicity. The identification of mycobacterial species is now rapid and relatively simple. Some of the pathogens identified as causative agents are used as a designation of the disease (e.g. cutaneous *Mycobacterium massiliense* infection).

Clinical symptoms of cutaneous NTM infection

A number of cutaneous diseases, such as erythema, nodules, erosion and ulcers, have been attributed to NTM infection. The point of entry is thought to be via minute cutaneous wounds in which bacteria are attached. Although a visceral NTM infection may cause cutaneous infection in immunocompromised patients, it is not yet clear how many bacteria are required for pathogenicity. There is usually only one cutaneous lesion; however, multiple skin lesions have been observed when pathogenic microbes spread through the lymph fluid. Most infected skin lesions are on exposed areas such as the hands, feet or face, supporting the premise that small external wounds are the penetration pathway. For example, in cutaneous *M. marinum* infection, also known as fish tank granuloma, approximately 80% of the patients have eruption(s) in finger, hand and/or wrist joints. Patients do not experience the pain or itching usually associated with eruptions, but inflammation does sometimes lead to tenderness and/or spontaneous pain.^{11,12}

Correspondence: Kazue Nakanaga, Ph.D., Department of Mycobacteriology, Leprosy Research Center, National Institute of Infectious Diseases, 4-2-1 Aoba, Higashi-Murayama, Tokyo 189-0002, Japan. Email: nakanaga@nih.go.jp
Received 7 September 2011; accepted 24 October 2012.

Table 1. Causative agents of cutaneous mycobacterial infections

Growth rate	Traditional Runyon classification	Species (<i>Mycobacterium</i>)	Disease
Slow growers	<i>M. tuberculosis</i> complex	<i>M. tuberculosis</i> <i>M. bovis</i>	Cutaneous tuberculosis
	Group I Photochromogens	<i>M. kansasii</i> <i>M. marinum</i> <i>M. simiae</i>	Non-tuberculous mycobacterial infection
	Group II Scotochromogens	<i>M. goodii</i> <i>M. scrofulaceum</i> <i>M. szulgai</i> <i>M. ulcerans</i> subsp. <i>shinshuense</i> ^a <i>M. ulcerans</i> ^a	
	Group III Non-photochromogens	<i>M. avium</i> <i>M. haemophilum</i> <i>M. intracellulare</i> <i>M. xenopi</i> ^b	
Rapid growers	Group IV Rapid growers	<i>M. abscessus</i> <i>M. chelonae</i> <i>M. fortuitum</i> <i>M. peregrinum</i> <i>M. vaccae</i>	
Unculturable in artificial medium		<i>M. leprae</i>	Hansen's disease (Leprosy)

^aYellow pigmentation is sometimes lost after several passages. ^bNon-pigmented colonies during early growth. However, most colonies become yellow with age.

CONVENTIONAL IDENTIFICATION OF CUTANEOUS NTM

Specimens

Pus or skin exudate, skin scrapings and skin biopsies are the major source of samples used to perform both conventional and molecular mycobacterial assays (Table 2).^{13,14} Isolates, formalin-fixed and/or formalin-fixed paraffin-embedded sections are also used for analysis. Animal coats, aquatic animals, seawater, tap water and swimming pool water are also used in the search for sources of infection. To date, we have received 90 clinical specimens (swabs and tissues) for NTM detection and identification, 225 cultured colonies for identification, 31 paraffin-embedded specimens for detection and 278 NTM cultured colonies for drug susceptibility assay from April 2009 to March 2011. As we discuss later, we have been using this pipeline since 2006, and these samples were analyzed at least in part to reach the correct identification.

Smear test and pathological test

Swabs containing pus or skin exudate spread on a slide glass is used for the smear tests. Smears are stained (Ziehl-Neelsen [Z-N] or Auramine O staining) and examined by light microscopy or fluorescent microscopy (Fig. 1). Pathology specimens are also stained with Z-N staining (Fig 2).

Culture test

Liquid or solid medium is used to culture samples obtained from swabs containing pus or exudate, skin brushes and skin biopsies. The major liquid medium has a Middlebrook 7H9

Broth base combined with a growth indicator system (Mycobacteria Growth Indicator Tube, MB/BacT).^{15,16} Three representative solid media are the egg-based Löwenstein-Jensen,

Table 2. Laboratory procedures to detect and identify cutaneous NTM

Pus or scrapings
PCR
Smear test (Z-N stain)
Culture at room temperature: L-J or Ogawa medium
Culture at 37°C: liquid medium (e.g. MGIT)
Frozen in -20°C
Biopsy samples
PCR
Pathological test (Z-N stain)
Culture at room temperature: L-J or Ogawa medium
Culture at 37°C: liquid medium (e.g. MGIT)
Frozen in -20°C
PCR
Culture
Cultured samples
PCR
DDH
Biochemical assays
Drug susceptibility assays
Paraffin- embedded materials
PCR

DDH, DNA-DNA hybridization; L-J medium, Löwenstein-Jensen medium; MGIT, Mycobacteria Growth Indicator Tube;¹⁵ NTM, non-tuberculous mycobacterial; PCR, polymerase chain reaction; Z-N stain, Ziehl-Neelsen stain.

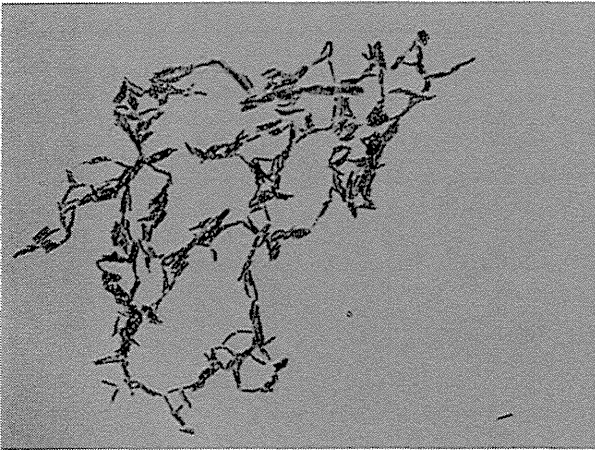


Figure 1. Smear Ziehl-Neelsen staining (original magnification $\times 1000$).

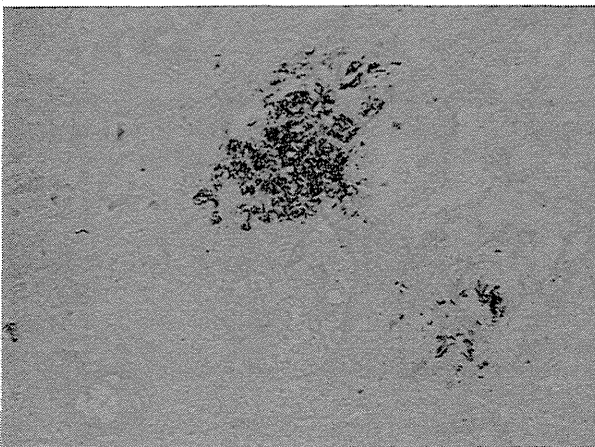


Figure 2. Pathological Ziehl-Neelsen staining (original magnification $\times 400$).

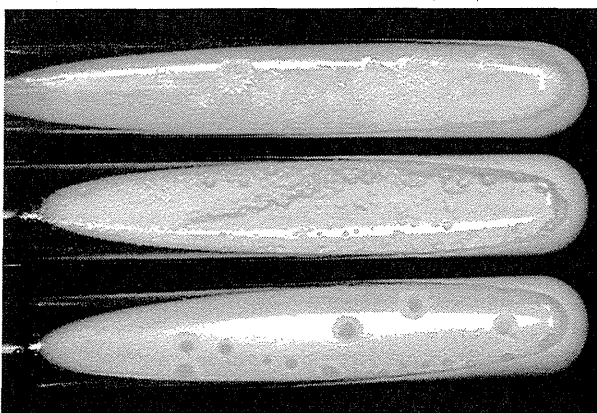


Figure 3. Ogawa medium (culture positive).

Ogawa medium (Fig. 3), or Middlebrook 7H10/7H11 agar medium.¹⁷ Before culturing, pretreatment with Nalc-NaOH is necessary to avoid contamination by other bacteria or fungi. Optimal culturing temperature varies depending on species: 40°C, 37°C, 33°C, 30°C, 28°C and room temperature are frequently used. If multiple incubators are not available for simultaneous use, incubation at 37°C is recommended with simultaneous culturing at room temperature. The isolation period of the causative agents may be shortened when liquid media is used. However, the shortened growth period may not allow sufficient time to observe colony characteristics. Because liquid medium is not suitable for identification when samples contain multiple pathogens, it is recommended that both liquid and solid cultures be grown at the same time.

Biochemical analysis

Biochemical analyses such as the niacin and catalase tests and other enzymatic reaction assays have been the most frequently performed procedures for mycobacterial species identification. These biochemical tests have certain limitations that lead some laboratories to avoid them. For example, testing can only be performed after successful isolation. In addition, running the tests requires complicated quality control and technical expertise.^{13,14}

MOLECULAR IDENTIFICATION OF CUTANEOUS NTM

Differential diagnosis by DNA-DNA hybridization (DDH) assays

Differential diagnosis using a commercial kit for mycobacterial DDH can be performed when bacterial isolates are available.¹⁸ The kit contains a panel of 18 major mycobacteria (Table 3). However, it is impossible to diagnose a rare species and subspecies that is not included in the panel, and there have

Table 3. Mycobacterial species identifiable in a commercially available DNA-DNA hybridization test

TB complex (<i>M. africanum</i> , <i>M. bovis</i> , <i>M. microti</i> , <i>M. tuberculosis</i>)
<i>M. abscessus</i>
<i>M. avium</i>
<i>M. chelonae</i>
<i>M. fortuitum</i>
<i>M. gastri</i>
<i>M. gordonae</i>
<i>M. intracellulare</i>
<i>M. kansasii</i>
<i>M. marinum</i>
<i>M. nonchromogenicum</i>
<i>M. peregrinum</i>
<i>M. scrofulaceum</i>
<i>M. simiae</i>
<i>M. szulgai</i>
<i>M. terrae</i>
<i>M. triviale</i>
<i>M. xenopi</i>

been several cases of false positives. Attempts to differentiate *Mycobacterium ulcerans* subsp. *shinshuense* (the causative agent of Buruli ulcer [BU] in Japan)⁹ from *M. ulcerans* using this kit yield an identification of *M. marinum* (Fig. 4).¹⁹ *Mycobacterium massiliense* and *Mycobacterium bolletii* are misidentified as *Mycobacterium abscessus*,²⁰ while *Mycobacterium heckeshornense* is classified as *Mycobacterium xenopi*. Additional laboratory procedures are required to discriminate these species. Polymerase chain reaction (PCR) detection of insertion sequence (IS)2404 can be used to differentiate *M. ulcerans* and/or *M. ulcerans* subsp. *shinshuense* from *M. marinum*.^{9,19} However, combination sequence analysis using the *hsp65* and *rpoB* genes is required to separate *M. abscessus*, *M. massiliense* and *M. bolletii*.²⁰

Gene amplification assays

Diagnostic genotyping kits for the detection of pathogenic mycobacterial genomes such as *M. tuberculosis*, *Mycobacterium avium*, *Mycobacterium intracellulare* and *Mycobacterium kansasii* are commercially available.^{21–23} The correct results

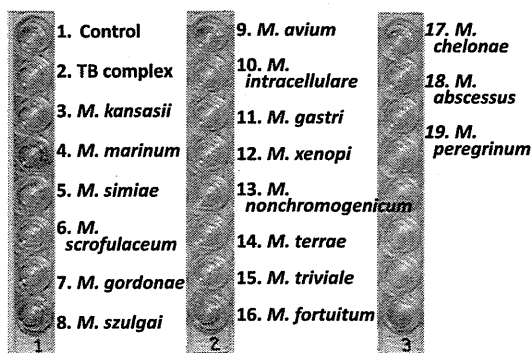


Figure 4. Commercially available DNA–DNA hybridization assay using an *Mycobacterium ulcerans* subsp. *shinshuense* clinical isolate. Blue color change was observed in a well of *M. marinum*.

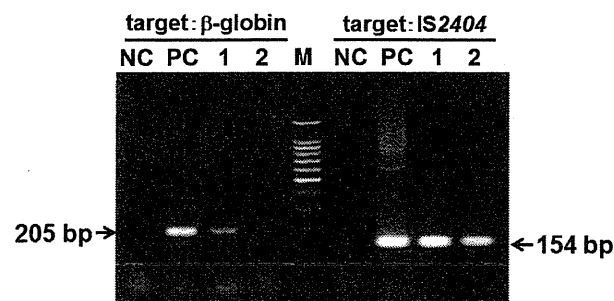


Figure 5. Gel electrophoresis of polymerase chain reaction products amplified using template DNA extracted from formalin-fixed and paraffin-embedded sections. 1, sample 1; 2, sample 2; NC, negative control; PC, positive control.

can be rapidly obtained if certain mycobacteria are present in the specimen material. However, when the results are negative, the smear test and/or culture assays should be performed for the other NTM.

Culturing an SGM can take several weeks. Therefore, genotyping assays such as species-specific PCR (Fig. 5) or 16S rRNA gene sequencing (described below) are extremely effective. Even for RGM species such as *Mycobacterium chelonae*, *M. abscessus* or *Mycobacterium fortuitum*, the primary isolation takes several weeks, but identification can be hastened using genotypic assays in parallel with culture assays. Specimens are sometimes processed into formalin-fixed paraffin-embedded blocks or frozen embedded blocks, making culture assays impossible. The sensitivity and specificity of PCR from these blocks is variable, depending on the condition of the DNA in the specimens. The order of preferred samples for genotypic analysis (from best to worst) is: cultured colonies > fresh specimens > ethanol-fixed specimens > formalin-fixed paraffin-embedded specimens.

Identification using the 16S rRNA gene sequence

If an abundance of bacterial DNA is available, sequence analysis of the first one-third of the 16S rRNA gene (Table 4, primer set; 8F16S-1047R16S) can be used for strain comparisons in the Ribosomal Differentiation of Medical Micro-organisms (RIDOM) database (www.ridom-rdna.de/).^{29–31} RIDOM uses the sequence text to find the top 10 reference strains with the highest homology to the query sequence. The sequences contain approximately 500 bp, which includes hypervariable regions A and B of the mycobacterial 16S rRNA gene (*E. coli* positions 54–510). Sequence homology greater than 99% usually leads to a call that two strains are identical. However, this method cannot differentiate between *M. ulcerans* subsp. *shinshuense*, *M. marinum* and *M. ulcerans* due to their sequence similarity. In other cases, *M. kansasii* and *Mycobacterium gastri* exhibit 100% homology in the first 500 bp of their 16S rRNA genes, as do members of the *M. chelonae-abscessus* group.^{32,33} These strains require additional methods for differentiation. Sequence analysis of the majority of the 16S rRNA gene (1500 bp) allows differentiation of *M. ulcerans* subsp. *shinshuense*, *M. marinum* and *M. ulcerans* (Table 5).^{19,34} The longer sequence read also distinguishes *M. chelonae* from the rest of the *M. chelonae-abscessus* group. Still, even this methodology cannot differentiate between *M. abscessus*, *M. bolletii* and *M. massiliense*.²⁰ There are other databases such as the Ez Taxon identification service (EzTaxon-e) and the basic local alignment search tool (BLAST), but they have no quality control standards for the submission of reference sequences.^{35,36}

Identification using other housekeeping gene sequences

The sequence of the 16S rRNA gene (first one-third) cannot identify or differentiate some mycobacterium strains, but the entire gene is relatively large, and large amounts of DNA template are required to obtain the entire sequence. A more sensitive method for the targeting of multiple housekeeping genes

Table 4. Primers used for NTM and *M. ulcerans* detection and identification

Primer	Sequence	Target and/or purpose (amplified fragment size)	Reference
8F16S	5'-AGAGTTTGATCCTGGCTCAG-3' (positions 8 to 27) ^a	Mycobacterial 16S rRNA gene, PCR (1500 bp), sequencing	24
1047R16S	5'-TGCACACAGGCCACAAGGGA-3' (positions 1047 to 1028) ^a		
830F16S	5'-GTGTGGGTTTCTTCCTTGG-3' (positions 830 to 849) ^a		
1542R16S	5'-AAGGAGGTGATCCAGCCGCA-3' (positions 1542 to 1523) ^a		
TB11	5'-ACCAACGATGGTGTGTCAT-3'	Mycobacterial <i>hsp65</i> gene, PCR (441 bp), sequencing	25
TB12	5'-CTTGTCGAACCGCATACCCT-3'		
MabrpoF	5'-GAGGGTCAGACCACGATGAC-3' (positions 2112–2131) ^b	Mycobacterial <i>rpoB</i> gene, PCR (449 bp), sequencing	20
MabrpoR	5'-AGCCGATCAGACCGATGTT-3' (positions 2559–2541) ^b		
MF	5'-CGACCACTTCGGCAACCG-3'	Mycobacterial <i>rpoB</i> gene, PCR (341 bp), sequencing	26
MR	5'-TCGATCGGGCACATCCGG-3'		
ITSF	5'-TTGTACACACCGCCCGTC-3'	Mycobacterial 16S-23S ITS region, PCR (340 bp), sequencing	27
ITSR	5'-TCTCGATGCCAAGGCATCCACC-3'		
PU4F	5'-GCGCAGATCAACTTCGCGGT-3'	<i>M. ulcerans</i> IS2404, PCR (154 bp)	28
PU7Rbio	5'-GCCCGATTGGTGCTCGGTCA-3'		

^aNucleotide positions were assigned using the coli *E. coli* 16S rRNA gene sequence as a reference. ^bPrimer design and nucleotide positions were based on the *M. tuberculosis rpoB* gene sequence (Genbank accession no. L27989). ITS, internal transcribed spacer; PCR, polymerase chain reaction.

Table 5. 16S rRNA gene sequences differentiating *Mycobacterium ulcerans* and related species¹⁹

Organism	Origin	492 ^a	1247	1288	1449–1451
<i>M. ulcerans</i> subsp. <i>shinshuense</i> ATCC 33728	Japan	GGGGA	GTGCA	AAGGC	ACCC—TTTG
<i>M. ulcerans</i> subsp. <i>shinshuense</i> LRC 0501	Japan	GGGGA	GTGCA	AAGGC	ACCC—TTTG
<i>M. ulcerans</i> ITM 98–912	China	GGGGA	GTGCA	AAGGC	ACCC—TTTG
<i>M. ulcerans</i> Agy99	Ghana	GGAGA	GTGCA	AACGC	ACCCTTTTTG
<i>M. ulcerans</i> ATCC 19423 ^T	Australia	GGAGA	GTGCA	AACGC	ACCC—TTTG
<i>M. ulcerans</i> 1615	Malaysia	GGAGA	GTGCA	AACGC	ACCC—TTTG
<i>M. ulcerans</i> 5143	Mexico	GGAGA	GTGCA	AAAGC	ACCC—TTTG
<i>M. marinum</i> ATCC 927 ^T	USA	GGAGA	GTACA	AAAGC	ACCC—TTTG

^aNucleotide position(s) were based on *Escherichia coli* 16S rRNA gene sequence. Underline indicated differing residue(s).

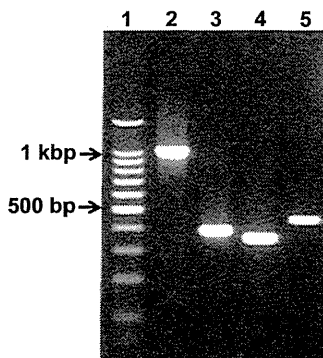


Figure 6. Gel electrophoresis of polymerase chain reaction products from skin biopsy specimens using a 2% agarose gel. Lane 1, 100-bp ladder; lane 2, 16S rRNA gene (8F16S-1047R16S); lane 3, internal transcribed spacer region; lane 4, *rpoB* gene (MF-MR); lane 5, *hsp65* gene.

for PCR and sequence analysis was required.³⁷ In addition to the 16S rRNA gene, we analyzed the DNA sequences of heat shock protein 65 (*hsp65*), *rpoB* and the 16S–23S intergenic spacer region (ITS region). Table 4 shows the sets of primers applicable to most strains of mycobacterium. Figure 6 shows the result of gel electrophoresis analysis after PCR using template DNA extracted from regions of affected skin and primers for the 16S rRNA gene (8F16S-1047R16S), the ITS region, *rpoB* (MF-MR) and *hsp65*. This figure shows amplified single bands; however, extra bands or inadequate amplification are sometimes apparent. The *rpoB* gene is the most polymorphic of the regions examined and is, therefore, very useful for identification, but the acquisition of PCR products is relatively difficult and the preparation of two different primer sets (MabrpoF-MabrpoR and MF-MR) is required to achieve the desired results. RIDOM database analysis using sequences of the ITS region and the 16S rRNA gene will find strains with higher levels of homology. In contrast, a BLAST search of *rpoB*